Theoretical Study on the Structures and Stability of SiC_3P Isomers

Hui-ling Liu,[†] Xu-ri Huang,*[,†] Guang-hui Chen,[†,‡] Yi-hong Ding,[†] and Chia-chung Sun[†]

State Key Laboratory of Theoretical and Computational Chemistry, Institute of Theoretical Chemistry, Jilin University, Changchun 130023, People's Republic of China, and Department of Chemistry, Mudanjiang Normal College, Mudanjiang 157012, People's Republic of China

Received: August 12, 2004; In Final Form: October 20, 2004

Various levels of calculations are applied to obtain the structures, energies, dipole moments, vibrational spectra, rotational constants, and isomerization of SiC_3P species. A total of 27 minima which are connected by 40 interconversion transition states on the potential energy surface are located at the DFT/B3LYP/6-311G(d) level. The global minimum is found to be a linear SiCCCP of the $^2\Pi$ electronic state. Besides the three-membered-ring isomer CC-cCPSi (36.2 kcal/mol), the four-membered-ring isomers P-cCCCSi (31.2 kcal/mol) and P-cSiCCC (79.1 kcal/mol), the five-membered-ring isomer cCPCCSi (46.6 kcal/mol), and the cagelike isomer pPSiCCC (56.8 kcal/mol) also possess great kinetic stability (more than 10.0 kcal/mol). The bonding natures of the relevant species are analyzed. The calculated results may be helpful for understanding the P-doped SiC vaporization process. The structures, energies, and bonding properties of the relevant species are compared with those of the SiC_2N, SiC_2P, and SiC_3N analogues.

1. Introduction

Silicon, carbon, and phosphorus chemistry have received considerable attention from various aspects. One of the particular interests is their possible role in astrophysical chemistry. Up to now, several silicon-, carbon-, or phosphorus-containing molecules, such as SiC_n ($n = 1-4$), SiN, SiO, SiS, PC, PN, and even $HC_{11}N$, have been detected in interstellar space.[1] The SiCN radical in an astronomical source has been detected, and the microwave spectrum of it was reported in the laboratory.[2]

On the other hand, Si- or P-containing species have been believed to play an important role in material chemistry. Binary silicon carbides are commonly used in microelectronic and photoelectronic applications.[3] P-doped SiC compounds are generally used as semiconducting materials,[4] while the Si−P bond can be found in various fields such as inorganic, organic, and organometallic chemistry.[5] Recently, the hydrogenated SiCP ion has recently been prepared by deposition with properly activated silane−propyne−phosphine mixtures.[6]

Recently, molecules containing Si, N, or P atoms, that is, Si_2P_2,[7] SiC_2N,[8] SiC_2P,[9] and SiC_3N,[10] have been extensively investigated. At the same time, theoretical and experimental investigations on the species SiC_n, C_nN, and C_nP ($n = 1-3$) have been widely reported.[11] The mixture of them, that is, SiC_nX (X = N or P) species, may present a bridge between the SiC_n and C_nX (X = N or P) clusters. Understanding the structures, bonding, and stabilities of the SiC_nX (X = N or P) series may be helpful for future identification of the new Si-, C-, N-, or P-containing species either in the laboratory or in interstellar space and also for elucidation of the N- or P-doped SiC material formation mechanism. Here, we chose to study the SiC_3P radical that is chemically isovalent to SiC_3N, whose potential energy surface (PES) has been achieved in our previous research.[8] Theoretical investigations have shown that, for SiC_2N, only chainlike structures are kinetically stable, yet SiC_2P and SiC_3N radicals have not only chainlike structures but also cyclic structures as kinetically stable isomers. Some discrepancies and similarities must exist among the SiC_nX system, so we wonder whether SiC_3P has stable cyclic structures and even cagelike structures to be allowed in the experimental or interstellar observation.

2. Computational Methods

All computations are carried out with the GAUSSIAN 98[12] and MOLCAS 5.2[13] (for CASSCF and CASPT2) program packages. The optimized geometries and harmonic vibrational frequencies of the local minima and transition states are obtained at the DFT/B3LYP/6-311G(d)[14] theory level. To get reliable relative energies, the CCSD(T)/6-311G(2d)[15] single-point energy calculations are further performed including the zero-point vibrational energies (ZPVEs) using the DFT/B3LYP/6-311G(d) geometries. To confirm whether the obtained transition states connect to the right isomers, the intrinsic reaction coordinate (IRC)[16] calculations are performed at the DFT/B3LYP/6-311G(d) level. Further, for the relevant species, the structures and frequencies are refined at the QCISD/6-311G(d)[17] level and the single-point energies at the CCSD(T)/6-311G(2df)//QCISD/6-311G(d)+ZPVE and CCSD(T)/cc-pVTZ//DFT/B3LYP/cc-pVTZ+ZPVE levels. Also, the CASPT2(13,13)/6-311G(2df)//CASSCF(13,13)/6-311G(2df) calculations are used to check relevant species' multiconfigurational effects. Unless otherwise specified, the relative energies (in kilocalories per mole) are at the CCSD(T)/6-311G(2d)//DFT/B3LYP/6-311G(d)+ZPVE level (simplified as CCSD(T)//DFT/B3LYP).

3. Results and Discussions

Including as many isomeric forms as possible, we initially considered five types of isomers, that is, chainlike species (I), three-membered-ring species (II), four-membered-ring species (III), five-membered-ring species (IV), and cagelike species (V), which are shown in Figure 1. After numerous searches, a total

[†] Jilin University.
[‡] Mudanjiang Normal College.

10.1021/jp046348o CCC: $27.50
Published on Web 12/03/2004

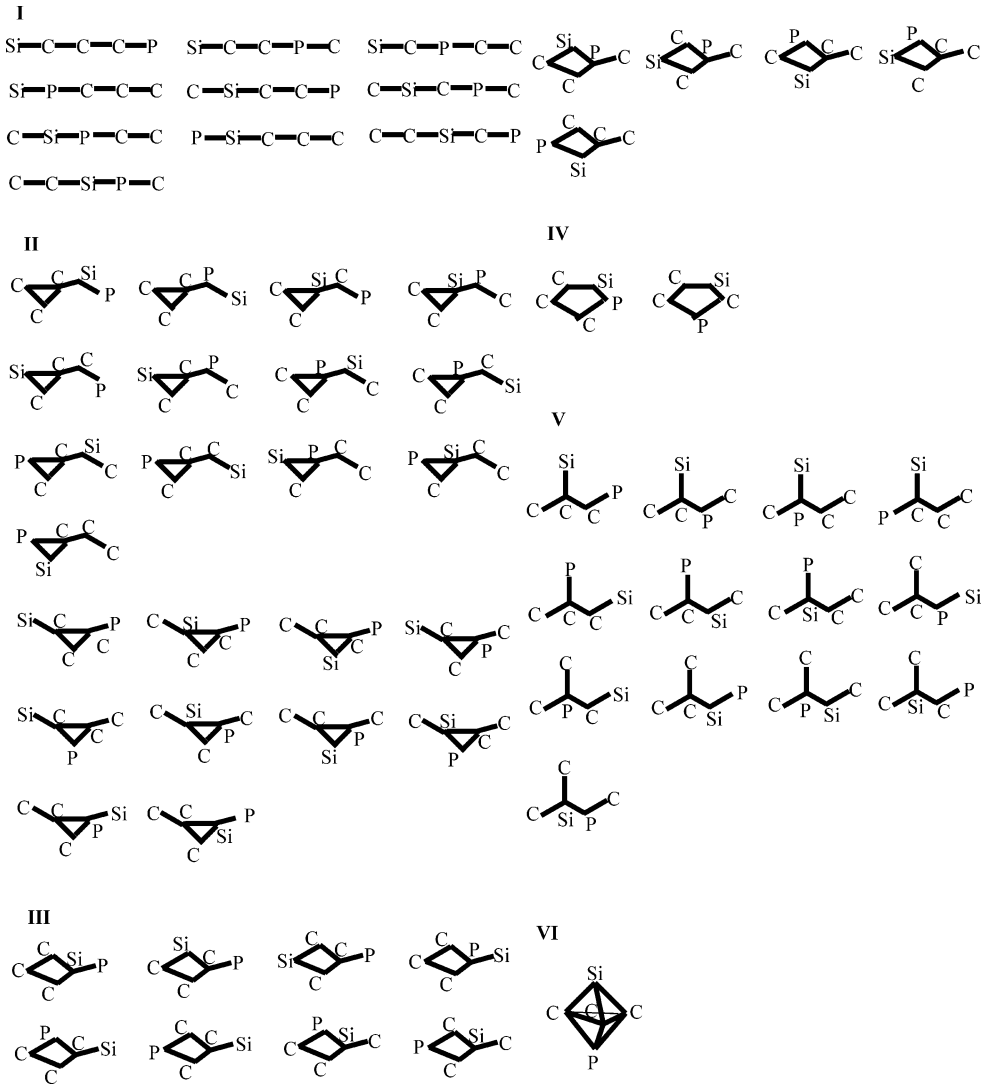

Figure 1. Scheme for isomeric species search.

of 27 minima (**m**) connected by 40 interconversion transition states (**TSm/n**) were located, and the structures of them are shown in Figures 2 and 3, respectively. The harmonic vibrational frequencies as well as the infrared intensities, dipole moments, and rotational constants of relevant species at the DFT/B3LYP/6-311G(d), QCISD/6-311G(d), and DFT/B3LYP/cc-pVTZ levels are listed in Table 1. The relative energies of isomers and transition states at various levels are summarized in Table 2. The possible dissociation products' energies are shown in Table 3, and the corresponding structures are shown in Figure 4. A schematic potential energy surface (PES) of SiC_3P is depicted in Figure 5.

3.1. SiC_3P Species. On the potential energy surface (PES), a total of eight chainlike isomers are located. The lowest-lying isomer is linear SiCCCP **1** (0.0), and the other linear one CCCSiP **4** (73.0) has a higher energy; both are of the $^2\Pi$ electronic state. Among the six bent species, CCCPSi **3** (64.1) and CSiCCP **8** (98.9) are of the $^2A''$ electronic state, while CCPCSi **5** (73.7), CCPCSi **6** (75.9), and CPCCSi **7** (83.1) are of the $^2A'$ electronic state. The remaining isomer CCSiCP **2** (48.4) is of C_1 symmetry.

There are five isomers that possess three-membered rings. Among them, PC-cCCSi **9** (14.0) and PC-cSiCC **11** (46.2) have SiCC rings, whereas CC-cCPSi **10** (36.2) and CC-cSiCP **12** (70.5) have SiCP rings. All of the above four isomers are of C_s symmetry with the $^2A'$ electronic state, while PSi-cCCC **13** (83.1) is C_{2v} symmetrized with the $^2B_2$ electronic state.

Four isomers can be located as minima with four-membered-ring structures, all of which are C_{2v} symmetrized with the $^2B_2$ electronic state. Among these isomers, P-cCCCSi **14** (31.2), P-cSiCCC **16** (79.1), and P-cSiCCC **17** (92.7) all have SiCCC rhombic rings, while Si-cCCCP **15** (56.9) has a CCCP rhombic ring structure. Isomers **14**, **15**, and **16** have CC cross-bonding, while isomer **17** has CSi cross-bonding.

For the six five-membered-ring isomers, cCPCCSi **18** (46.6) and cPCCCSi **19** (50.0) containing CC cross-bonding are C_s symmetrized with the $^2A''$ electronic state. cCCCPSi **20** (50.5) has CC and CSi cross-bondings. cCCPCSi **21** (53.6), cCCPCSi **22** (65.4), and cCCCPSi **23** (67.9) have CSi, CP, and CC cross-bondings, respectively.

All the remaining four isomers including pCCCSiP **24** (51.5), pPSiCCC **25** (56.8), pCCCPSi **26** (60.7), and pCCPCSi **27** (65.9) possess cagelike structures. Isomers **24** and **25** are of C_s symmetry with the $^2A''$ and $^2A'$ electronic states, respectively. Both isomers **26** and **27** are of C_1 symmetry.

The isomerization process of the SiC_3P isomers on the PES is depicted in Figure 5. For the reason that the lowest isomerization or dissociation barriers control the kinetic stability of isomers, we need to consider as many as possible isomerization and dissociation pathways. As shown in Table 3, the

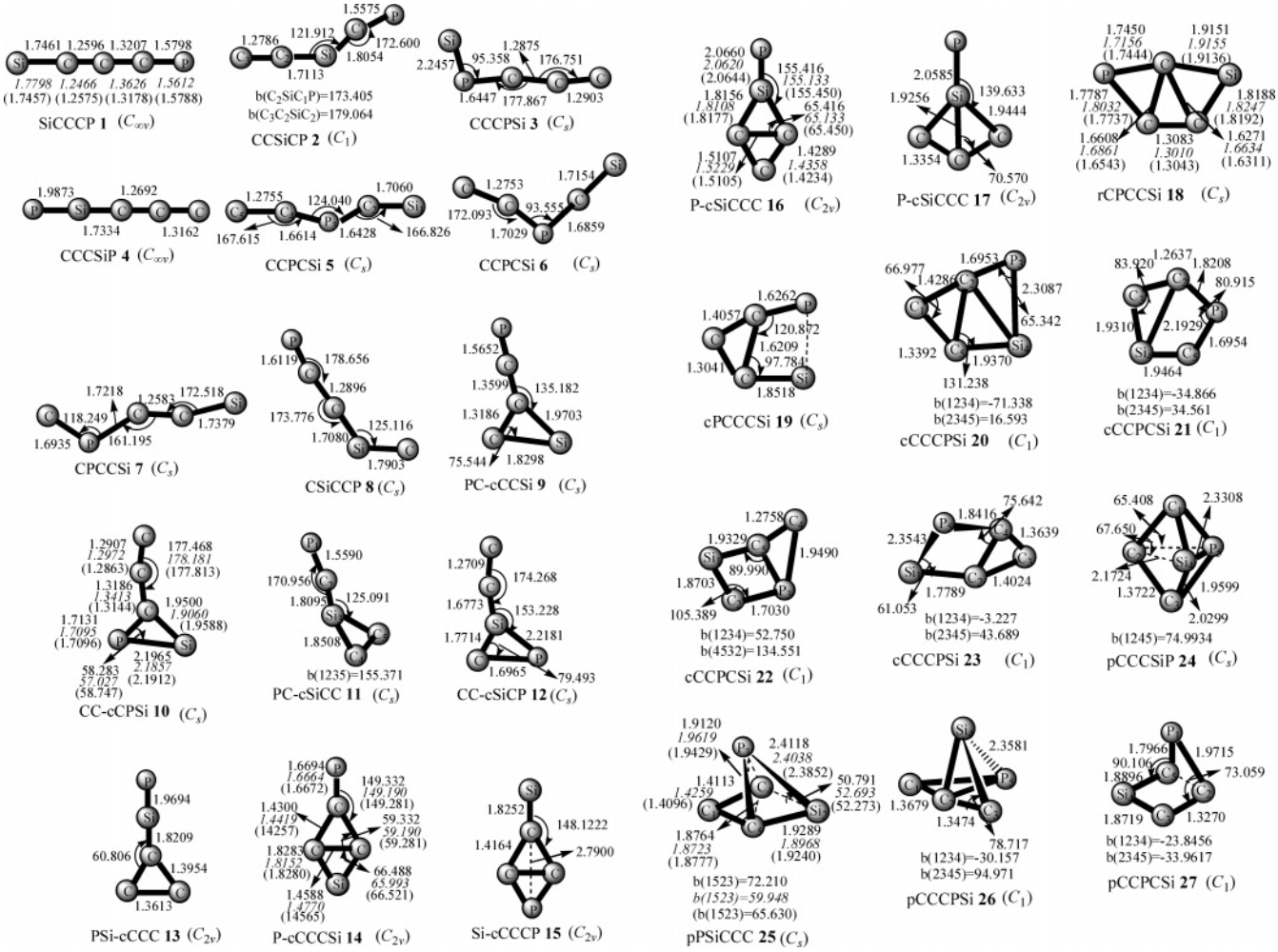

Figure 2. Optimized geometries of SiC_3P isomers at the DFT/B3LYP/6-311G(d) level. Bond lengths are in angstroms and angles in degrees. The values obtained at the QCISD/6-311G(d) level and with the DFT/B3LYP/cc-pVTZ method for some relevant isomers are also given in italics and in parentheses, respectively.

relative energies of the dissociation products are so high (more than 100 kcal/mol at the CCSD(T)//DFT/B3LYP level) that we do not attempt to search any dissociation transition states. Thus, it is the isomerization barriers that control the kinetic stability of SiC_3P isomers. At the CCSD(T)/6-311G(2d) level, the linear SiCCCP **1** is the lowest-lying energy isomer with a large kinetic stability of 14.6 (*16.0*) (**1** → **9**) kcal/mol. The italic values in parentheses are obtained at the CCSD(T)//QCISD level. Both four-membered-ring species **14** (31.2) and **16** (79.1) have large kinetic barriers of 15.6 (*17.1*) (**14** → **9**) and 15.2 (*12.2*) (**16** → **13**) kcal/mol, respectively. At the QCISD/6-311G(d) level, isomer **13** cannot be located as a minimum with all real frequencies. The respective kinetic stabilities of **10** (36.2) and **18** (46.6) are 10.0 (*8.3*) (**10** → **1**) and 10.1 (*11.8*) (**18** → **21**) kcal/mol. Such kinetic stabilities are high enough to allow the existence of them under low-temperature conditions (such as in dense interstellar clouds). As for the cagelike structure **25** (56.8), the kinetic stability is high at 11.5 (*11.7*) (**25** → **27**) kcal/mol. Apart from isomers **1**, **10**, **13**, **14**, **16**, **18**, and **25**, the other isomers have much lower kinetic stabilities. At the CCSD(T)//DFT/B3LYP level, the smaller isomerization barriers of the remaining species are −0.7 (**2**, **2** → **11**), 8.2 (**4**, **4** → **10**), 8.4 (**8**, **8** → **9**), 0.6 (**9**, **9** → **1**), 1.5 (**11**, **11** → **2**), 7.4 (**12**, **12** → **2**), 6.3 (**15**, **15** → **18**), 4.2 (**17**, **17** → **4**), 9.0 (**19**, **19** → **1**), 8.3 (**20**, **20** → **1**), 3.1 (**21**, **21** → **18**), 1.4 (**22**, **22** → **21**), 2.9 (**23**, **23** → **10**), 9.4 (**24**, **24** → **26**), 0.2 (**26**, **26** → **24**), and 2.4 (**27**, **27** → **25**). Still, no transition states relative to isomers **3** (64.1), **5** (73.7), **6** (75.9), and **7** (83.1) can be located. For their high energies, the four isomers mentioned above may be of minute importance as observable species either in the laboratory or in interstellar space.

It should be pointed out that the CP radical and cyclic SiC_2 and SiC_3 molecules have been detected in interstellar space. Adding the P atom directly to the cyclic SiC_3 molecule may possibly lead to isomers **14**, **16**, **18**, and **25**. Attaching the CP radical to the cyclic SiC_2 molecule can initially generate the high-energy isomer PC-cSiCC **11**, which is able to change to **1** (CP + SiC_2 → **11** → **2** → **9** → **1**) through the complex isomerization channels.

3.2. Properties of the Relevant Species. In section 3.1, we know that only the six isomers **1**, **10**, **14**, **16**, **18**, and **25** possess both considerable kinetic and thermodynamic stabilities and may be detected in the laboratory and in interstellar space. We now analyze their structures and bonding natures at the DFT/B3LYP/6-311G(d) level.

The lowest-energy isomer SiCCCP **1** corresponding to the $^2\Pi$ electronic state possesses the dominant electronic configuration $1\sigma^2 2\sigma^2 3\sigma^2 4\sigma^2 5\sigma^2 1\pi^4 6\sigma^2 2\pi^4 3\pi^1$. The 5σ and 6σ molecular orbitals are essentially atomic orbitals belonging to the terminal Si and P. The low-lying 1π orbital spreads over the whole molecule with most on CCCP, while the 2π orbital is mainly delocalized over the terminal CP with little on SiCC. Its SiC bond length (1.7461 Å) is longer than the SiC double (1.7071 Å) bond, while the CC bond connecting to the Si atom (l.2596

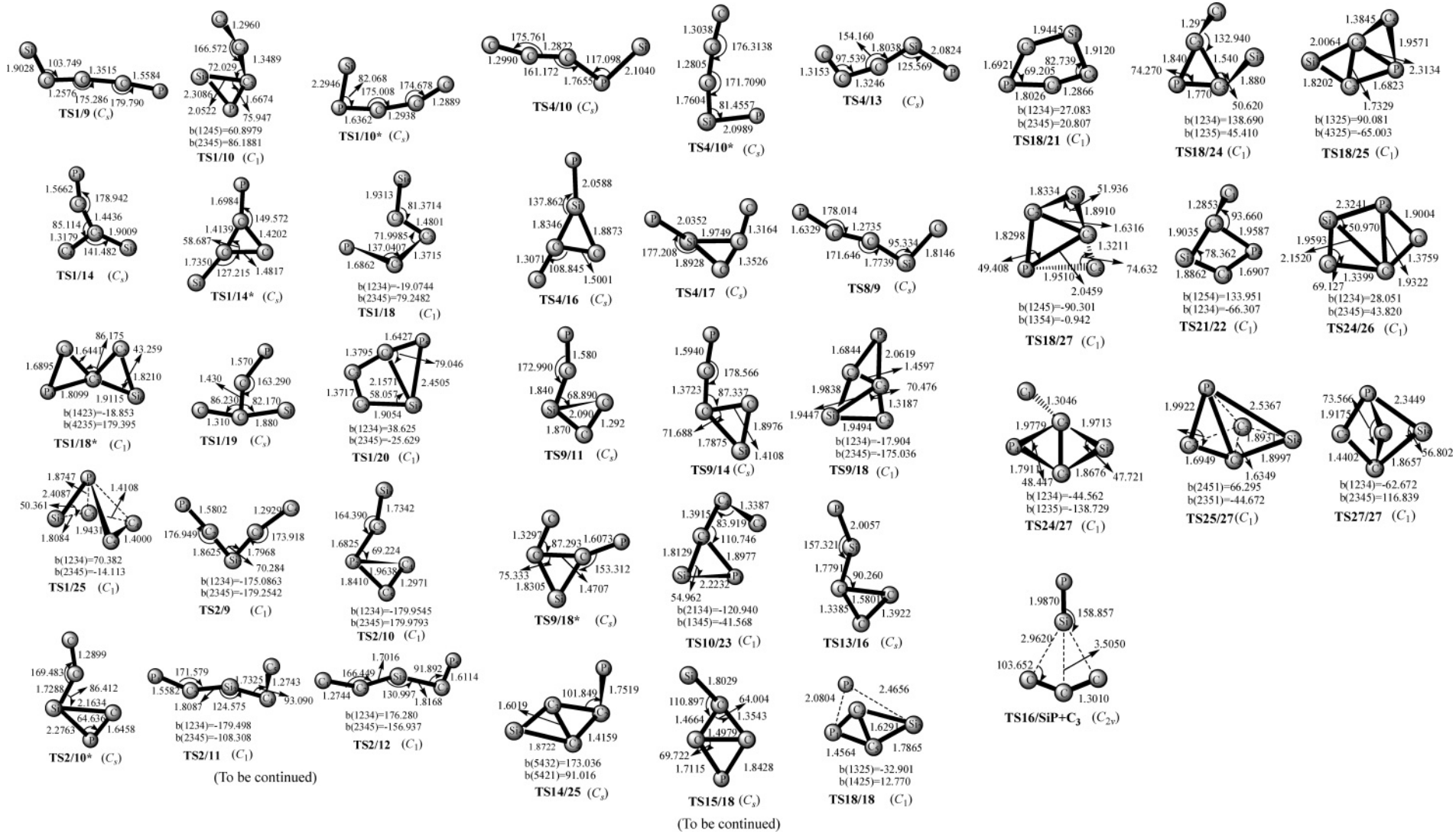

Figure 3. Optimized geometries of interconversion transition states between SiC_3P isomers at the DFT/B3LYP/6-311G(d) level. Bond lengths are in angstroms and angles in degrees.

TABLE 1: Harmonic Vibrational Frequencies (cm^{-1}), Infrared Intensities (km/mol) (in Parentheses), Dipole Moments (D), and Rotational Constants (GHz) of the Relevant SiC_3P Structures at the DFT/B3LYP/6-311G(d), QCISD/6-311g(d), and DFT/B3LYP/cc-pVTZ Levels

species	frequencies (cm^{-1}) ($km \cdot mol^{-1}$)	dipole moment (D)	rotational constant
SiCCCP **1**	85 (1) 101 (2) 245 (0) 297 (0) 450 (8) 474 (4) 553 (6) 874 (2) 1571 (112) 1884 (1)	0.5367	0.914 108
SiCCCP **1**[a]	77 (2) 95 (2) 171 (2) 212 (0) 320 (2) 423 (9) 423 (6) 855 (11) 1534 (194) 1877 (11)	0.0225	0.900 225
SiCCCP **1**[b]	84 (1) 100 (1) 244 (0) 296 (0) 449 (8) 486 (7) 564 (8) 871 (3) 1568 (94) 1876 (1)	0.5132	0.916 229
CC-cCPSi **10**	115 (3) 170 (2) 344 (6) 434 (4) 435 (2) 520 (65) 632 (8) 1305 (1) 1929 (547)	4.8122	7.085 67, 2.409 23, 1.797 92
CC-cCPSi **10**[a]	103 (4) 165 (1) 350 (8) 415 (2) 446 (0) 590 (57) 667 (30) 1254 (4) 1897 (497)	4.6678	7.174 14, 2.390 83, 1.793 23
CC-cCPSi **10**[b]	116 (3) 177 (3) 347 (5) 440 (2) 482 (2) 518 (67) 633 (7) 1314 (1) 1929 (590)	4.9594	7.115 60, 2.417 76, 1.804 59
P-cCCCSi **14**	157 (3) 209 (5) 473 (40) 474 (13) 479(0) 881 (62) 984 (0) 1030 (23) 1479 (97)	1.6941	39.580 39, 1.568 76, 1.508 95
P-cCCCSi **14**[a]	155 (4) 214 (5) 476 (0) 484 (8) 490 (38) 909 (103) 1026 (0) 1040 (24) 1494 (96)	1.6620	38.609 27, 1.575 85, 1.514 05
P-cCCCSi **14**[b]	157 (2) 209 (4) 473 (12) 478 (45) 484 (0) 882 (67) 981 (0) 1028 (19) 1475 (84)	1.6506	39.702 90, 1.573 57, 1.513 58
P-cSiCCC **16**	99 (9) 125 (7) 352 (1) 424 (47) 438(2) 724 (7) 891 (40) 1029 (18) 1419 (172)	3.2002	36.909 65, 1.713 15, 1.637 16
P-cSiCCC **16**[a]	106 (9) 135 (9) 353 (1) 453 (1) 466 (37) 758 (10) 932 (79) 1063 (16) 1438 (244)	3.4061	36.318 94, 1.721 27, 1.643 38
P-cSiCCC **16**[b]	113 (10) 133 (7) 350 (1) 432 (44) 442 (3) 727 (6) 889 (38) 1030 (19) 1415 (177)	3.5023	36.919 38, 1.714 91, 1.638 79
cCPCCSi **18**	213 (4) 266 (6) 291 (11) 451 (46) 489 (1) 593 (16) 770 (63) 937 (18) 1560 (41)	0.4988	14.525 27, 2.453 80, 2.099 18
cCPCCSi **18**[a]	215 (4) 265 (5) 294 (16) 453 (26) 512 (1) 620 (58) 764 (71) 980 (132) 1556 (11)	0.5441	13.864 65, 2.490 88, 2.111 53
cCPCCSi **18**[b]	215 (4) 277 (6) 290 (10) 439 (42) 488 (2) 593 (10) 769 (64) 936 (13) 1563 (39)	0.4515	14.584 44, 2.457 76, 2.103 31
pPSiCCC **25**	122 (1) 288 (8) 433 (14) 519 (21) 520 (9) 583 (17) 734 (9) 951 (13) 1282 (32)	1.4191	7.005 24, 4.504 71, 3.556 97
pPSiCCC **25**[a]	240 (6) 259 (6) 395 (10) 562 (9) 585 (29) 609 (13) 759 (21) 1108 (4) 1310 (13)	1.2678	7.481 02, 4.432 45, 3.622 60
pPSiCCC **25**[b]	65 (0) 295 (8) 399 (12) 523 (7) 535 (23) 574 (15) 721 (12) 984 (10) 1303 (24)	1.3658	7.149 99, 4.518 98, 3.604 49

[a] At the QCISD/6-311G(d) level. [b] At the DFT/B3LYP/cc-pVTZ level.

Å) is just between the CC double (1.3269 Å) and triple (1.1981 Å) bond values.[18] The other CC bond length (1.3207 Å) is very close to the normal CC double bond, and the CP bond length (1.5798 Å) is slightly longer than the CP triple bond (1.5392 Å). Coupled with the orbital analysis, isomer **1** can be described as the following resonant structures: (1) •|Si−C≡C−C≡P|, (2) |Si=C=C•−C≡P|, and (3) |Si=C=C=C=P|• (where "|" denotes the lone electron pair and "•" denotes the single electron). The atomic spin densities (0.585, −0.138, 0.304, −0.168, and 0.416 e for Si, C, C, C, and P, respectively) suggest that structure 1 bears the most weight and structure 2 the least.

For the three-membered-ring isomer **10**, the dominant configuration is $1a'^2 2a'^2 3a'^2 4a'^2 5a'^2 1a''^2 6a'^2 7a'^2 8a'^2 2a''^2 9a'^1$. It has two sets of π orbitals, 1a″ and 2a″. The low-lying 1a″ orbital spreads over the whole molecule with most on the PCCC and little on Si, while the high-lying 2a″ orbital is mainly on the CPSi three-membered ring with little on the terminal CC bond. Both of the two CC bonds (1.2907 and 1.3186 Å for the terminal and the internal, respectively) are shorter than the typical CC double bond (1.3269 Å). The CP and PSi bonds (1.7131 and 2.1965 Å) are slightly shorter than the normal CP double (1.7183 Å) and PSi single (2.2832 Å) bonds, respectively. The CSi bond value (1.9500 Å) is longer than the normal CSi single bond (1.8851 Å). Coupled with the orbital analysis, the bonding nature of isomer **10** can be viewed as resonant structures among the following three modes:

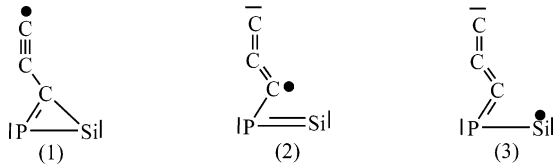

The spin densities (0.446, 0.126, 0.172, 0.058, and 0.198 e for C, C, C, P, and Si, respectively) suggest that mode 1 bears the most weight and mode 2 the least.

The four-membered-ring structure P-cCCCSi **14** of C_{2v} symmetry with the $^2B_2$ electronic state has the electronic configuration $1a_1^2 2a_1^2 3a_1^2 1b_2^2 1b_1^2 4a_1^2 2b_2^2 5a_1^2 6a_1^2 2b_1^2 3b_2^1$. The $1b_1$ π orbital spreads all over the five atoms with most on the CCC ring, while the other two sets of π orbitals, $2b_2$ and $2b_1$, are delocalized mainly on the terminal PC bond with little on the CCSi ring. The $5a_1$ molecular orbital represents basically a lone electron pair of the Si atom, whereas the $6a_1$ molecular orbital can be associated with the CC cross-bond. As for the unpaired electron, it mainly stays on the phosphorus 3p orbital. Its terminal PC bond length (1.6694 Å) is shorter than the typical PC double bond (1.7183 Å). The peripheral CC, CSi, and the CC cross-bond lengths are 1.4300, 1.8283, and 1.4588 Å, respectively, just between the single and double CC and CSi bond lengths. The spin densities (0.994, −0.087, 0.045, 0.003, and 0.045 e for P, C, C, Si, and C along clockwise order, respectively), bond lengths, and orbital analysis of isomer **14** suggest a main structure such as

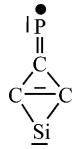

Another kinetically stable isomer, **16**, of C_{2v} symmetry with the $^2B_2$ electronic state, possessing a SiCCC four-membered ring just like isomer **14**, has the structural character of the P atom connecting to a Si atom different from the structure of isomer **14**. Its electronic configuration can be described as $1a_1^2 2a_1^2 3a_1^2 1b_2^2 4a_1^2 1b_1^2 2b_2^2 5a_1^2 6a_1^2 2b_1^2 3b_2^1$. The $1b_1$ π orbital is delocalized over the entire molecule with most on the SiCCC ring, and the $2b_1$ orbital is mainly delocalized over the terminal PSi bond with little on the CCC. The $6a_1$ orbital can be associated with the CC cross-bond, and the unpaired electron is mainly a phosphorus 3p orbital. The peripheral CC, SiC, and CC cross-bond lengths (1.4289, 1.8156, and 1.5107 Å, respectively) are close to those of isomer **14**. The terminal SiP bond length (2.0660 Å) is very close to the typical SiP double bond (2.0812 Å). The bond lengths and the orbital analysis suggest a main structure such as

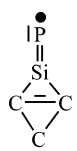

TABLE 2: Relative Energies (kcal/mol) of the SiC_3P Isomers and Transition States at the DFT/B3LYP/6-311G(d) and Single-Point CCSD(T)/6-311G(2d) Levels[a]

species	B3LYP[b]	ΔZPVE B3LYP[b]	CCSD(T)[c] //B3LYP[b]	total 1	QCISD[b]	ΔZPVE QCISD[b]	CCSD(T)[d] //QCISD[b]	total 2	B3LYP[e]	ΔZPVE B3LYP[e]	CCSD(T)[e] //B3LYP[e]	total 3	CASPT2// CASSCF[f]
SiCCCP **1**[g]($^2\Pi$)	0.0	0.0	0.0	0.0	0.0	0.0	0.0	0.0	0.0	0.0	0.0	0.0	0.0
CCSiCP **2**	56.5	−1.5	49.9	48.4									
CCCPSi **3**(^{2}A″)	64.6	−1.1	65.2	64.1									
CCCSiP **4**($^2\Pi$)	75.6	−1.4	74.4	73.0									
CCPCSi **5**(^{2}A′)	77.2	−1.7	75.4	73.7									
CCPCSi **6**(^{2}A′)	79.2	−1.9	77.8	75.9									
CPCCSi **7**(^{2}A′)	89.1	−2.4	85.5	83.1									
CSiCCP **8**(^{2}A″)	102.0	−2.1	101.0	98.9									
PC-cCCSi **9**(^{2}A′)	19.1	−0.3	14.3	14.0	10.3	0.6	11.8	12.4	18.8	−0.3	13.1	12.8	12.0
CC-cCPSi **10**(^{2}A′)	38.7	−0.9	37.1	36.2	36.7	−0.1	34.0	33.9	35.1	−0.8	33.5	32.7	34.4
PC-cSiCC **11**(^{2}A′)	59.0	−1.7	47.9	46.2									
CC-cSiCP **12**(^{2}A′)	79.5	−1.4	71.9	70.5									
PSi-cCCC **13**($^2B_2$)	88.7	−2.2	85.3	83.1									
P-cCCCSi **14**($^2B_2$)	37.6	−0.5	31.7	31.2	27.0	0.4	27.9	28.3	36.9	−0.5	28.3	27.8	27.1
Si-cCCCP **15**($^2B_2$)	61.6	−1.4	58.3	56.9									
P-cSiCCC **16**($^2B_2$)	88.9	−1.5	80.6	79.1	78.3	−0.4	74.6	74.2	84.8	−1.4	72.7	71.7	76.0
P-cSiCCC **17**($^2B_2$)	101.7	−2.0	94.7	92.7									
cCPCCSi **18**(^{2}A″)	54.4	−1.4	48.0	46.6	43.1	−0.5	41.4	40.9	52.6	−1.4	41.4	40.0	39.6
cPCCCSi **19**(^{2}A″)	59.7	−1.1	51.1	50.0									
cCCCPSi **20**	58.2	−1.3	51.8	50.5									
cCCPCSi **21**	66.6	−1.2	54.8	53.6									
cCCPCSi **22**	78.3	−1.5	66.9	65.4									
cCCCPSi **23**	78.3	−2.0	69.9	67.9									
pCCCSiP **24**(^{2}A″)	64.7	−1.1	52.6	51.5									
pPSiCCC **25**(^{2}A′)	71.0	−1.6	58.4	56.8	59.2	−0.2	49.3	49.1	67.5	−1.6	49.0	47.4	44.8
pCCCPSi **26**	73.6	−1.4	62.1	60.7									
pCCPCSi **27**	79.9	−1.7	67.6	65.9									
TS1/9(^{2}A′)	31.4	−0.5	15.1	14.6	23.7	0.2	15.8	16.0	31.0	−0.6	24.4	23.8	
TS1/10	52.5	−1.6	47.8	46.2	49.6	−0.7	42.9	42.2	47.4	−1.5	41.9	40.4	
TS1/10*(^{2}A″)	64.9	−1.2	56.3	55.1									
TS1/14(^{2}A′)	68.8	−1.9	60.5	58.6									
TS1/14*(^{2}A′)	65.6	−1.7	62.4	60.7									
TS1/18	79.7	−1.9	67.9	66.0									
TS1/18*	93.3	−2.5	85.3	82.8									
TS1/19(^{2}A″)	69.0	−1.9	60.9	59.0									
TS1/20	69.1	−1.7	60.5	58.8									
TS1/25	83.7	−2.3	72.9	70.6									
TS2/9	68.0	−2.3	63.2	60.9									
TS2/10	91.5	−2.5	84.1	81.6									
TS2/10*(^{2}A′)	103.4	−2.9	96.2	93.3									
TS2/11	60.0	−1.7	49.4	47.7									
TS2/12	88.6	−2.2	80.1	77.9									
TS4/10(^{2}A′)	77.7	−1.6	82.8	81.2									
TS4/10*(^{2}A″)	85.9	−1.4	85.6	84.2									
TS4/13(^{2}A′)	101.1	−2.3	106.2	103.9									
TS4/16(^{2}A′)	125.5	−2.9	127.7	124.8									
TS4/17(^{2}A′)	104.3	−2.4	99.3	96.9									
TS8/9(^{2}A′)	107.3	−2.2	109.5	107.3									
TS9/11(^{2}A′)	72.7	−2.3	64.5	62.2									
TS9/14(^{2}A′)	53.2	−1.6	48.4	46.8	45.2	−0.8	46.2	45.4	52.9	−1.7	46.1	44.4	
TS9/18	68.9	−1.9	62.2	60.3									
TS9/18*(^{2}A″)	74.7	−1.5	67.2	65.7									
TS10/23	81.4	−1.9	72.7	70.8									
TS13/16(^{2}A′)	97.3	−2.1	96.4	94.3	93.7	−1.6	88.0	86.4	94.2	−2.1	86.8	84.7	
TS14/25(^{2}A′)	103.1	−1.9	95.3	93.4									
TS15/18(^{2}A″)	69.5	−1.7	64.9	63.2									
TS18/18	80.4	−2.5	67.1	64.6									
TS18/21	68.4	−1.9	58.6	56.7	65.3	−1.0	53.7	52.7	56.1	−1.9	53.4	51.5	
TS18/24	79.2	−2.0	68.2	66.2									
TS18/25	89.0	−2.4	76.9	74.5									
TS18/27	82.1	−2.3	71.3	69.0									
TS21/22	80.3	−1.9	68.7	66.8									
TS24/26	74.4	−1.9	62.8	60.9									
TS24/27	82.2	−2.0	70.8	68.8									
TS25/27	82.4	−2.1	70.4	68.3	69.2	−1.2	62.0	60.8	78.5	−2.2	61.5	59.3	
TS27/27	101.0	−2.4	87.9	85.5									
TS16/SiP+CCC ($^2A_1$)	135.0	−2.9	123.3	120.4									

[a] For the relevant isomers, the CCSD(T)/6-311G(2df)//QCISD/6-311G(d), CCSD(T)/cc-pVTZ//DFT/B3LYP/cc-pVTZ, and CASPT2(13,13)/6-311G(2df)//CASSCF(13,13)/6-311G(2df) values are included also. [b] The basis set is 6-311G(d) for DFT/B3LYP and QCISD. [c] The basis set is 6-311G(2d) for CCSD(T). [d] The basis set is 6-311G(2df) for CCSD(T). [e] The basis set is cc-pVTZ for DFT/B3LYP and CCSD(T). [f] The 6-311G(2df) basis set and 13*13 electrons and active orbitals are used for the CASSCF and CASPT2 methods. [g] The total energy of reference isomer **1** at the DFT/B3LYP/6-311G(d) level is −745.083 971 9 au, at the CCSD(T)/6-311G(2d)//DFT/ B3LYP/6-311G(d) level is −743.815 039 3 au, at the QCISD/6-311G(d) level is −743.732 305 5 au, at the CCSD(T)/6-311G(2df)//QCISD/6-311G(d) level is −743.879 874 au, and at the CASPT2//CASSCF(13,13) level is −744.156 913 4 au. The ZPVEs at the DFT/B3LYP and QCISD levels are 0.014 884 and 0.013 641 au, respectively. The symbols in parentheses in this column denote the electronic states.

TABLE 3: Relative Energies (kcal/mol) of the Possible Dissociation Products of SiC_3P Isomers at the DFT/B3LYP/6-311G(d) and Single-Point CCSD(T)/6-311G(2d) Levels[a]

species	B3LYP[b]	ΔZPVE B3LYP[b]	CCSD(T)[c]// B3LYP[b]	total
$Si(^1D)+PCCC(^2\Pi)$[d]	148.8	−1.8	134.4	132.6
$Si(^3P)+PCCC(^2\Pi)$	122.8	−1.8	110.3	108.5
$Si(^1D)+C\text{-}cPCC(^2A')$	266.7	−2.2	242.5	240.3
$Si(^3P)+C\text{-}cPCC(^2A')$	240.7	−2.2	218.4	216.2
$Si(^1D)+CPCC(^2A')$	236.2	−3.7	221.2	217.5
$Si(^3P)+CPCC(^2A')$	210.2	−3.7	197.1	193.4
$C(^1D)+SiCPC(^2A')$	288.4	−4.7	263.7	259.0
$C(^3P)+SiCPC(^2A')$	246.4	−4.7	227.5	222.8
$C(^1D)+SiCCP(^2\Pi)$	199.3	−3.0	177.7	174.7
$C(^3P)+SiCCP(^2\Pi)$	157.3	−3.0	141.5	138.5
$C(^1D)+PSiCC(^2\Pi)$	253.6	−4.0	247.6	243.6
$C(^3P)+PSiCC(^2\Pi)$	211.5	−4.0	211.4	207.4
$C(^1D)+CSiCP(^2A')$	282.0	−4.5	250.9	246.4
$C(^3P)+CSiCP(^2A')$	240.0	−4.5	214.7	210.2
$C(^1D)+P\text{-}cSiCC(^2B_1)$	251.0	−4.0	224.2	220.2
$C(^3P)+P\text{-}cSiCC(^2B_1)$	208.9	−4.0	188.0	184.0
$C(^1D)+Si\text{-}cPCC(^2B_1)$	275.2	−4.8	277.4	272.6
$C(^3P)+Si\text{-}cPCC(^2B_1)$	233.1	−4.8	241.2	236.4
$C(^1D)+cCCPSi\ 3(^2A'')$	212.8	−3.6	185.1	181.5
$C(^3P)+cCCPSi\ 3(^2A'')$	170.8	−3.6	148.9	145.3
$C(^1D)+cCCPSi\ 3'(^2A'')$	228.3	−4.0	201.5	197.5
$C(^3P)+cCCPSi\ 3'(^2A'')$	186.2	−4.0	165.3	161.3
$C(^1D)+cCSiCP\ 4(^2B_1)$	217.6	−3.5	154.7	151.2
$C(^3P)+cCSiCP\ 4(^2B_1)$	175.6	−3.5	118.4	114.9
$C(^1D)+cCSiCP\ 4'(^2A'')$	251.9	−4.7	223.1	218.4
$C(^3P)+cCSiCP\ 4'(^2A'')$	209.9	−4.7	186.9	182.2
$C(^1D)+cCSiCP\ 5(^2A'')$	251.9	−4.7	223.1	218.4
$C(^3P)+cCSiCP\ 5(^2A'')$	209.8	−4.7	186.9	182.2
$C(^1D)+cCSiCP\ 5'(^2A_2)$	290.9	−5.0	275.5	270.5
$C(^3P)+cCSiCP\ 5'(^2A_2)$	248.9	−5.0	239.3	234.3
$P(^2D)+CSiCC(^1\Sigma)$	262.3	−3.9	220.4	216.5
$P(^4S)+CSiCC(^1\Sigma)$	223.7	−3.9	186.6	182.7
$P(^2D)+CSiCC(^3\Pi)$	263.3	−3.1	272.2	269.1
$P(^4S)+CSiCC(^3\Pi)$	224.7	−3.1	238.4	235.3
$P(^2D)+SiCCC(^1\Sigma)$	176.4	−2.2	159.1	156.9
$P(^4S)+SiCCC(^1\Sigma)$	137.8	−2.2	125.3	123.1
$P(^2D)+SiCCC(^3\Pi)$	155.1	−2.2	151.1	148.9
$P(^4S)+SiCCC(^1\Pi)$	116.5	−2.2	117.3	115.1
$P(^2D)+cSiCCC\ 1(^1A_1)$	169.1	−2.5	148.3	145.8
$P(^4S)+cSiCCC\ 1(^1A_1)$	130.5	−2.5	114.5	112.0
$P(^2D)+cSiCCC\ 1(^3B_1)$	186.6	−2.9	170.7	167.8
$P(^4S)+cSiCCC\ 1(^3B_1)$	148.0	−2.9	137.0	134.1
$P(^2D)+cSiCCC\ 2(^1A_1)$	173.8	−2.7	167.4	164.7
$P(^4S)+cSiCCC\ 2(^1A_1)$	135.2	−2.7	133.6	130.9
$P(^2D)+cSiCCC\ 2(^3B_1)$	180.4	−2.7	161.6	158.9
$P(^4S)+cSiCCC\ 2(^3B_1)$	141.8	−2.7	127.8	125.1
$CC(^1\Sigma_g)+SiPC(^2A')$	250.8	−4.6	259.5	254.9
$CC(^3\Pi_u)+SiPC(^2A')$	227.9	−4.9	293.5	288.6
$CC(^1\Sigma_g)+SiCP(^2\Pi)$	184.5	−3.5	144.7	141.2
$CC(^3\Pi_u)+SiCP(^2\Pi)$	161.5	−3.7	178.8	175.1
$CC(^1\Sigma_g)+PSiC(^2\Pi)$	273.7	−4.6	305.2	300.6
$CC(^3\Pi_u)+PSiC(^2\Pi)$	250.8	−4.9	339.3	334.4
$SiC(^1\Sigma)+CPC(^2A'')$	289.7	−5.1	259.5	254.4
$SiC(^3\Pi)+CPC(^2A'')$	262.9	−5.3	304.3	299.0
$SiC(^1\Sigma)+CCP(^2\Pi)$	198.7	−5.1	175.2	170.1
$SiC(^3\Pi)+CCP(^2\Pi)$	173.5	−3.6	220.0	216.4
$PC(^2\Sigma)+SiCC(^1\Sigma)$	141.2	−3.8	108.5	104.7
$PC(^2\Sigma)+SiCC(^3\Pi)$	187.4	−3.6	154.0	150.4
$PC(^2\Sigma)+SiCC(^1A_1)$	142.5	−3.9	107.1	103.2
$PC(^2\Sigma)+SiCC(^3B_2)$	180.9	−3.8	147.8	144.0
$PSi(^1\Sigma)+CCC(^1\Sigma_g)$	135.7	−3.3	124.0	120.7
$PSi(^1\Sigma)+CCC(^3\Pi_u)$	184.3	−5.0	179.0	174.0

[a] The $^3P-^1D$ experimental energy gaps of C and Si are 29.0 and 17.9 kcal/mol, respectively, and the $^4S-^2D$ experimental energy gap of P is 32.4 kcal/mol.[19] [b] The basis set is 6-311G(d) for DFT/B3LYP. [c] The basis set is 6-311G(2d) for CCSD(T). [d] The total energies of reference isomer **1** at the DFT/B3LYP and single-point CCSD(T) levels as well as the ZPVE at the DFT/B3LYP level are listed in footnote *g* of Table 2. The symbols in parentheses in this the column denote the electronic states.

The atomic spin densities (0.949, −0.014, 0.031, 0.003, and 0.031 e for P, Si, C, C, and C along clockwise order, respectively) confirm this conclusion.

The five-membered-ring species cCPCCSi **18** has the electronic configuration $1a'^22a'^23a'^24a'^25a'^21a''^26a'^27a'^28a'^22a''^23a''^1$. The 1a″ π orbital spreads over all the ring members, the 2a″ π orbital mainly is on the P_3C_4, while little is on the other three atoms. Its 8a′ orbital is associated with the C_1-C_4 cross-bond. Both of the CC cross-bond lengths (1.6271 Å for the one close to the Si atom and 1.6608 Å for the other) are longer than the CC single bond. Its peripheral CC bond (1.3083 Å) is shorter than the CC double bond. The two CP bonds (1.7450 Å for the one connecting to the Si atom and 1.7787 Å for the other) are between the single and double CP bond lengths. There are significant differences between the two SiC bonds, with the one connecting to the P atom (1.9151 Å) being longer and the other (1.8188 Å) being shorter than the normal SiC single bond. Together with the orbital analysis, isomer **25** can be described as the following resonant structures:

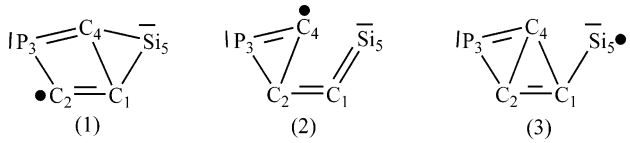

(1) (2) (3)

The spin densities (−0.066, 0.463, −0.136, 0.453, and 0.286 e for C_1, C_2, P_3, C_4, and Si_5, respectively) show that modes 1 and 2 bear somewhat more weight than mode 3.

Isomer **25** of C_s symmetry with the $^2A'$ electronic state, which can be viewed as a cagelike structure, possesses the electronic configuration $1a'^22a'^21a''^23a'^22a''^24a'^25a'^26a'^23a''^27a'^28a'^1$. The 1a″ π orbital spreads over the three C atoms, and the 2a″ π orbital spreads over all the atoms with most on the three C atoms. The 3a″ π orbital is mainly delocalized over $P_3-C_4-C_5$ with little on C_1 and Si_2. The length of the two CP bonds (1.9120 Å) is a little longer than the normal CP single bond (1.8730 Å). The bond length of SiP (2.4118 Å) is longer than the typical SiP single bond (2.2832 Å). The peripheral CC bond lengths (1.4113 Å) are just between typical CC single and double bonds. The two CSi bond values (1.9289 Å) are longer than the typical CSi single bond, while the CC cross-bond length (1.8764 Å) is longer than the CC single bond. Considering the orbital analysis, bond lengths, and spin densities (0.507, 0.175, 0.025, 0.146, and 0.146 e for C_1, Si_2, P_3, C_4, and C_5, respectively), we suggest the following resonant structures where structure 1 bears the most weight and structure 3 the least.

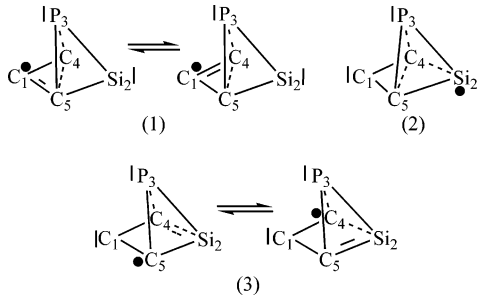

(1) (2) (3)

All the above bonding nature descriptions are confirmed by the natural bond orbital (NBO) analysis.

For the reason that the lowest-lying quartet linear state was found to lie more than 59 kcal/mol above $^2\Pi$ at correlated levels (CCSD(T)//DFT/B3LYP+ZPVE), the quartet species were not considered further. From Table 1, we can see that, at the QCISD/

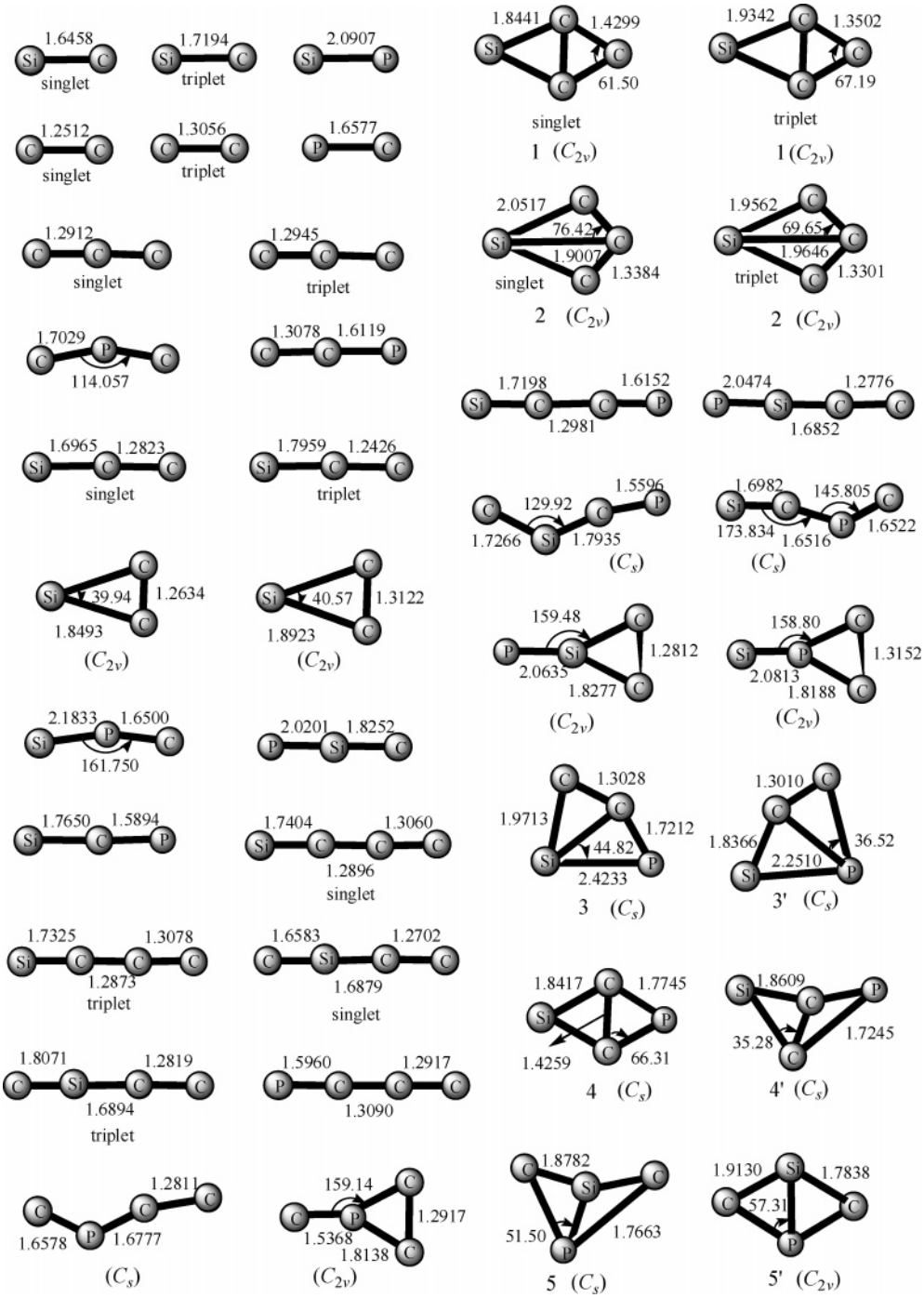

Figure 4. Optimized geometries of the possible dissociation products of SiC_3P isomers at the DFT/B3LYP/6-311G(d) level. Bond lengths are in angstroms and angles in degrees.

6-311G(d) level, the dipole moments of **1** and **18** are very small (0.0225 and 0.5441 D, respectively) and those of **10**, **14**, **16**, and **25** (4.6678, 1.6620, 3.4061, and 1.2678 D, respectively) are reasonable for microwave detection, yet isomers **1** and **18** can be identified by infrared spectrum. The dominant vibrational frequencies of isomers **1**, **10**, **14**, **16**, **18**, and **25** are 1877, 1897, 1494, 1438, 1556, and 1310 cm^{-1}, respectively, with the corresponding infrared intensities 11, 497, 96, 244, 11, and 13 km/mol. At the DFT/B3LYP/6-311G(d) level, the $\langle S^2 \rangle$ values are 0.7814, 0.7581, 0.7703, 0.7700, 0.7590, 0.7717, and 0.7558 for isomers **1**, **10**, **13**, **14**, **16**, **18**, and **25**, respectively, indicating that the spin contamination is small enough to be neglected. Moreover, the CASPT2//CASSCF calculations are performed to check the multiconfigurational properties of the above six isomers. The geometrical structures and relative energies at the CASPT2//CASSCF level are in good agreement with the DFT/B3LYP/6-311G(d) and QCISD/6-311G(d) results. The leading electronic configurations occupied by **1**, **10**, **14**, **16**, **18**, and **25** (82.26, 85.37, 84.96, 85.68, 84.23, and 84.47%, respectively) are the same as those that spanned the Slater determinant of DFT/B3LYP, indicating that the SiC_3P system has a negligible multiconfigurational effect and that the CCSD(T)//DFT/B3LYP method is adequate for calculation of the structures, vibrational spectra, and energies.

For the relevant species, the energies achieved at various levels (CCSD(T)/6-311G(2d)//DFT/B3LYP/6-311G(d), CCSD(T)/cc-pVTZ//DFT/B3LYP/ cc-pVTZ, and CCSD(T)/6-311G(2df)//QCISD/6-311G(d)) are different from each other among

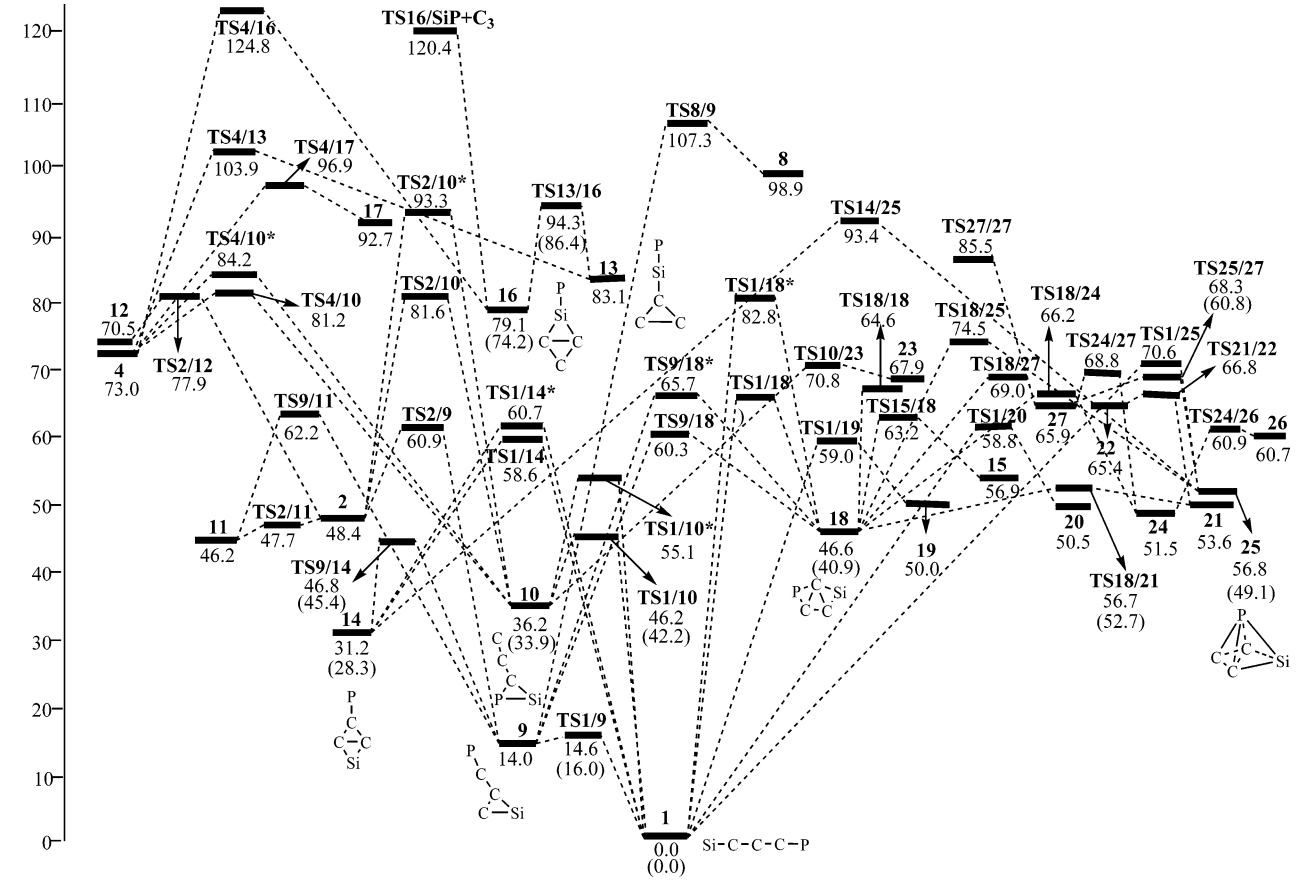

Figure 5. Schematic potential energy surface of SiC_3P at the CCSD(T)/6-311G(2d)//DFT/B3LYP/6-311G(d)+ZPVE level. The values in parentheses of the relevant species **1**, **14**, **16**, **10**, **18**, and **25** were obtained at the CCSD(T)/6-311G(2df)//QCISD/6-311G(d)+ZPVE level.

the levels, while the geometries and spectroscopies are very similar. In the view of the accuracy and computational cost, CCSD(T)//DFT/B3LYP/6-311G(d) is a reasonable level, while increasing the size of the basis set from 6-311G(d) to cc-pVTZ is also important for obtaining more reliable energies. Since the isomerization barrier of isomer **9** is enlarged to 11.0 kcal/mol at the CCSD(T)/cc-pVTZ//DFT/B3LYP/cc-pVTZ level, larger than those of the CCSD(T)//DFT/B3LYP/6-311G(d) and CCSD(T)//QCISD levels (0.6 and 3.6 kcal/mol, respectively), isomer **9** can be viewed as a stable structure with a CCSi three-membered ring and an exocyclic PCC bond at the DFT/B3LYP/cc-pVTZ level.

3.3. Comparison with Analogous SiC_2N, SiC_2P, and SiC_3N Species. Generally, isovalent or same series molecules are expected to possess similar chemical properties. However, there must be some discrepancies in the structures, bonding natures, and energies of SiC_2N, SiC_2P, SiC_3N, and SiC_3P, so it is attracting great interest to compare their special properties of structure, bonding, and PES.

The structures and stability of SiC_2N, SiC_2P, and SiC_3N radicals have been extensively studied.[8−10] The linear isomers SiCCN, SiCCP, and SiCCCN can be located as ground states on the PES of the SiC_2N, SiC_2P, and SiC_3N radicals, respectively. The dominant structure of SiCCN is |Si═C•—C≡N|, while that of SiCCP is between |Si═C═C═P|• and |Si═C•—C≡P|. The resonant structures of SiCCCN are between •|Si—C≡C—C≡N| and |Si═C═C•—C≡N|, while those of SiCCCP mentioned above are among •|Si—C≡C—C≡P|, |Si═C═C•—C≡P|, and |Si═C═C═C═P|•. Compared with SiCCN and SiCCCN which do not have |Si═C═C═N|• and |Si═C═C═C═N|•, the cumulene |Si═C═C═P|• and |Si═C═C═C═P|• structures of SiC_2P and SiC_3P may be due to the second-row P atom which shows much less of a trend to form a π bond than the corresponding first-row N atom. This difference between P and N atoms also leads to the reason that no linear isomers including an internal P atom can be located as kinetically stable structures in the SiC_2P and SiC_3P radicals, whereas linear isomers including an internal N atom can be located as kinetically stable ones in SiC_2N and SiC_3N radicals.

Besides chainlike structures, there are kinetically stable three-membered-ring and four-membered-ring structures on the SiC_2P and SiC_3N PESs, respectively. While, for the SiC_3P system, there are not only chainlike and cyclic structures but also kinetically stable cagelike structures. Compared with the C_2Si unit in SiC_2P, the tension decrease of the rhombic C_3Si unit in isomer **25** of SiC_3P may be the reason for the cagelike structure's large kinetic stability. Thus, no cagelike structures could be located as minima on the SiC_2P PES. At the same time, the first-row N atom of the penta-atomic radical SiC_3N has much less of a tendency to form σ bonds than the second-row P atom in SiC_3P, which could be the reason that the cagelike structures of SiC_3N are kinetically unstable.

4. Conclusions

Various methods are employed to study the structures, energies, dipole moments, rotational constants, and isomerization of the SiC_3P molecule. Among the 27 minimum isomers, only six isomers may be kinetically stable toward isomerization and dissociation. The lowest-energy isomer is found to be linear SiCCCP **1**, which can be described as a resonant structure among •|Si—C≡C—C≡P|, |Si═C═C•—C≡P|, and |Si═C═C═C═P|•. The addition of cyclic SiC_2 to the PC radical would generate isomer **1** through complex isomerization channels. It

should be noted that not only three-, four-, and five-membered-ring structures but also a cagelike structure, **25**, have been located as kinetically stable isomers on the PES, which also represents the first theoretical prediction that a cagelike form can exist in the SiC_nX series. Considering that the SiCN radical in an astronomical source has been detected and the hydrogenated SiCP ion has been prepared, SiC_3P as a promising interstellar molecule may be detected soon. The calculated spectroscopies of SiC_3P may be helpful for the future experimental and interstellar detection and also for understanding the initial step of the growing mechanism during the P-doped SiC vaporization process.

Acknowledgment. This work is supported by the National Natural Science Foundation of China (nos. 20073014 and 20103003), Excellent Young Teacher Foundation of the Ministry of Education of China, Excellent Young Foundation of Jilin Province, and Key Teacher Innovation Foundation of Universities of Heilongjiang Province. The authors are greatly thankful for the reviewers' invaluable comments.

Supporting Information Available: Tables showing the harmonic vibrational frequencies and corresponding infrared intensities of the unstable SiC_3P isomers at the DFT/B3LYP/6-311G(d) level and the relative energies of the quartet SiC_3P isomers which correspond to the relevant isomers in doublet at the DFT/B3LYP/6-311G(d) and single-point CCSD(T)/6-311G-(2d) levels. This material is available free of charge via the Internet at http://pubs.acs.org.

References and Notes

(1) (a) Winnewisser, G. *J. Mol. Struct.* **1997**, *408*/*409*, 1. (b) McCarthy, M. C.; Apponi, A. J.; Thaddeus, P. *J. Chem. Phys.* **1999**, *110*, 10645. (c) Apponi, A. J.; McCarthy, M. C.; Gottlieb, C. A.; Thaddeus, P. *J. Chem. Phys.* **1999**, *111*, 3911. (d) Bell, M. B.; Feldman, P. A.; Watson, J. K. G.; McCarthy, M. C.; Travers, M. J.; Gottlieb, C. A.; Thaddeus, P. *Astrophys. J.* **1999**, *518* (2), L740−747, Part 1.

(2) (a) Apponi, A. J.; McCarthy, M. C.; Gottlieb, C. A.; Thaddeus, P. *Astrophys. J.* **2000**, *536* (1), L55−58, Part 2. (b) Guelin, M.; Muller, S.; Cernicharo, J.; Apponi, A. J.; McCarhty, M. C.; Gottlieb, C. A.; Thaddeus, P. *Astron. Astrophys.* **2000**, *363* (1), L9−12. (c) McCarthy, M. C.; Apponi, A. J.; Gottlieb, C. A.; Thaddeus, P. *J. Chem. Phys.* **2001**, *115* (2), L870−877.

(3) Furthmller, J.; Bechstedt, F.; Hsken, H.; Schrter, B.; Richter, W. *Phys. Rev. B* **1998**, *58*, *13712*, L1.

(4) Carlsson, J. R. A.; Clevenger, L.; Hultman, L.; Li, X.-H.; Jordan-Sweet, J.; Lavie, C.; Roy, R. A.; Cabral, C., Jr.; Morals, G.; Ludwig, K. L.; Stephenson, G. B.; Hentzell, H. T. G. *Philos. Mag. B* **1997**, *75*, 363.

(5) Armitage, D. A. In *The Silicon-heteroatom Bond*; Patai, S., Rappoport, Z., Eds.; J. Wiley: New York, 1989; p 151; 1991, p 183.

(6) Operti, L.; Rabezzana, R.; Turco, F.; Vaglio, G. A. *J. Mass Spectrom.* **2004**, *39*, 682−690.

(7) Huang, X. R.; Ding, Y. H.; Li, Z. S.; Sun, C. C. *J. Phys. Chem. A* **2000**, *104*, 8765−8772.

(8) Ding, Y. H.; Li, Z. S.; Huang, X. R.; Sun, C. C. *J. Phys. Chem. A* **2001**, *105* (24), 5896−5901.

(9) Chen, G. H.; Ding, Y. H.; Huang, X. R.; Zhang, H. X.; Li, Z. S.; Sun, C. C. *J. Phys. Chem. A* **2002**, *106*, 10408−10414.

(10) Liu, H. L.; Huang, X. R.; Chen, G. H.; Ding, Y. H.; Sun, C. C. *J. Phys. Chem. A* **2004**, *108*, 6919.

(11) (a) Guelin, M.; Cernicharo, J.; Paubert, G.; Turner, B. E. *Astron. Astrophys.* **1990**, *230*, L9. (b) Bell, M. B.; Feldman, P. A.; Travers, M. J.; McCarthy, M. C.; Gottlieb, C. A.; Thaddeus, P. *Astrophys. J.* **1997**, *483*, 161. (c) Largo, A.; Barrientos, C.; Lopez, X.; Ugalde, J. M. *J. Phys. Chem.* **1994**, *98*, 3985. (d) del Rio, E.; Barientos, C.; Largo, A. *J. Phys. Chem.* **1996**, *100*, 585.

(12) Frisch, M. J.; Trucks, G. W.; Schlegel, H. B.; Scuseria, G. E.; Robb, M. A.; Cheeseman, J. R.; Zakrzewski, V. G.; Montgomery, J. A., Jr.; Stratmann, R. E.; Burant, J. C.; Dapprich, S.; Millam, J. M.; Daniels, A. D.; Kudin, K. N.; Strain, M. C.; Farkas, O.; Tomasi, J.; Barone, V.; Cossi, M.; Cammi, R.; Mennucci, B.; Pomelli, C.; Adamo, C.; Clifford, S.; Ochterski, J.; Petersson, G. A.; Ayala, P. Y.; Cui, Q.; Morokuma, K.; Malick, D. K.; Rabuck, A. D.; Raghavachari, K.; Foresman, J. B.; Cioslowski, J.; Ortiz, J. V.; Stefanov, B. B.; Liu, G.; Liashenko, A.; Piskorz, P.; Komaromi, I.; Gomperts, R.; Martin, R. L.; Fox, D. J.; Keith, T.; Al-Laham, M. A.; Peng, C. Y.; Nanayakkara, A.; Gonzalez, C.; Challacombe, M.; Gill, P. M. W.; Johnson, B. G.; Chen, W.; Wong, M. W.; Andres, J. L.; Head-Gordon, M.; Replogle, E. S.; Pople, J. A. *Gaussian 98*, revision A.6; Gaussian, Inc.: Pittsburgh, PA, 1998.

(13) Andersson, K.; Barysz, M.; Bernhardsson, A.; Blomberg, M. R. A.; Carissan, Y.; Cooper, D. L.; Cossi, M.; Fleig, T.; Fülscher, M. P.; Gagliardi, L.; Graaf, C. de; Hess, B. A.; Karlström, G.; Lindh, R.; Malmqvist, P.-Å.; Neogrády, P.; Olsen, J.; Roos, B. O.; Schimmelpfennig, B.; Schütz, M.; Seijo, L.; Serrano-Andrés, L.; Siegbahn, P. E. M.; Stålring, J.; Thorsteinsson, T.; Veryazov, V.; Wierzbowska, M.; Widmark, P.-O. *MOLCAS*, version 5.2; Lund University: Lund, Sweden, 2001.

(14) Becke, A. D. *J. Chem. Phys.* **1993**, *98*, 5648.

(15) Pople, J. A.; Head-Gordon, M.; Raghavachari, K. *J. Chem. Phys.* **1987**, *87*, 5968.

(16) (a) Gonzalez, C.; Schlegel, H. B. *J. Chem. Phys.* **1989**, *90*, 2154. (b) Gonzalez, C.; Schlegel, H. B. *J. Chem. Phys.* **1990**, *94*, 5523.

(17) (a) Gauss, J.; Cremer, C. *Chem. Phys. Lett.* **1988**, *150*, 280. (b) Trucks, G. W.; Frisch, M. J. Manuscript in preparation, 1998. (c) Salter, E. A.; Trucks, G. W.; Bartlett, R. J. *J. Chem. Phys.* **1989**, *90*, 1752.

(18) For parallel comparison, the following bond distances are calculated at the DFT/B3LYP/6-311G(d,p) (p for H atom) level (with frequency confirmation as stationary points) for the model systems SiH_3CH_3, SiH_2-CH_2, CSiH, CH_3CH_3, CH_2CH_2, CHCH, CH_3PH_2, CH_2PH, CHP, SiH_3PH_2, SiH_2PH, and SiHP, respectively: Si−C (1.8851 Å), Si═C (1.7071 Å), Si≡C (1.6020 Å), C−C (1.5305 Å), C═C (1.3269 Å), C≡C (1.1981 Å), C−P (1.8730 Å), C═P (1.7183 Å), C≡P (1.5392 Å), Si−P (2.2832 Å), Si═P (2.0812 Å), and Si≡P (1.9567 Å).

(19) United States Department of Commerce. *At. Energy Levels* **1949**, *1*, 163.